ISSN 0965-545X, Polymer Science, Series A, 2018, Vol. 60, No. 6, pp. 854–865. © Pleiades Publishing, Ltd., 2018.

COMPOSITES

Graphene Nanosheets Reinforced Epoxy Nanocomposites: Mechanical and Electrical Properties Evaluation[1]

F. Vahedi[a], M. Eskandarzade[b], K. Osouli-Bostanabad[c,d,e,*], and A. Tutunchi[e,]**

[a] *Engineering Department, Faculty of Engineering, Tarbiat Modares University, Tehran, Iran*

[b] *Mechanical Engineering Department, Faculty of Engineering, University of Mohaghegh Ardabili, Ardabil, Iran*

[c] *Research Center for Pharmaceutical Nanotechnology, Biomedicine Institute, Tabriz University of Medical Sciences, Tabriz, Iran*

[d] *Students Research Committee, Tabriz University of Medical Sciences, Tabriz, Iran*

[e] *Department of Materials Engineering, Institute of Mechanical Engineering, University of Tabriz, Tabriz, 51666-16444 Iran*

**e-mail: k_osouli@yahoo.com*

***e-mail: ab.tutunchi51@tabrizu.ac.ir*

Received May 13, 2018;
Revised Manuscript Received August 12, 2018

Abstract—Utilizing the direct mixing and conducting ultra-sonication with two solvent free and solvent-borne methods, Graphene nanosheets (GNSs)/Epoxy nanocomposites were fabricated through the present research. Mechanical and electrical properties of nanocomposites with various contents of GNSs were investigated. Mechanical properties such as tensile and flexural modulus, tensile and flexural strength were taken into account and the electrical conductivity was monitored throughout the tests. A considerable improvement in tensile modulus (12%) of the nanocomposites was observed using 0.5 wt % of GNSs and flexural modulus was enhanced by 10% in the presence of GNSs with the same filler contents. Moreover, flexural strength and tensile strength of the nanocomposites were improved by 5 and 15% at 0.1 wt %, respectively. In addition, the results revealed that the non-solvent method had a better effect on improving the mechanical properties rather than the solvent-borne method. Furthermore, the electrical conductivity was enhanced by increasing in GNSs contents, while the percolation threshold was at 1 wt %.

DOI: 10.1134/S0965545X18070064

INTRODUCTION

Nowadays, nanomaterials have gained many applications in various fields due to their exceptional structural properties which attracted scientist's interest to examine and develop the materials with enhanced physicochemical features, applicable in the field of nanotechnology with more dimensional stability. In this regard, carbon nanotubes (CNTs) have been produced by Iijima [1], polymer nanocomposites (PNCs) by Toyota Research Group [2] and Graphene (Gra) in 2004 by Andre Geim [3]. In particular, the PNCs discovery has opened the new horizons on the materials science field for applying various nanosized inorganic fillers (i.e. CNTs, carbon nanofibers (CNFs), magnetic nanoparticles [4–6], carbon black (CB), materials with natural origin, Gra and etc.) as the reinforcement components of polymeric composites with distinctive behaviors, which are potentially useful in numerous industries such as electronic, aerospace, automotive and construction [7–9]. Among different nanomaterials, which have been benefited in PNCs, the carbon based nanomaterials have some distinguished characteristics that make them proper candidates where an application needs good thermal and electrical conductivity properties along with the good mechanical performances.

Gra, which includes the exceptional mechanical properties, thermal and electrical conductivity, electromagnetic interference (EMI) shielding, more electron mobility in comparison with other allotropes of carbon such as exfoliated graphite, CNTs and CNFs, is an interesting material with honeycomb structure, one-atom-thick and two dimensional layers composed of sp^2-bonded carbon atoms [10–14]. It has been illustrated that mono-layered Gra has the following properties; ultimate tensile strength (130 ± 10GPa) [10, 11], Young's modulus ($\sim 1 \pm 0.1$ TPa) [10, 12], fracture strength ($\sim$125 GPa) [13], elastic modulus ($\sim$0.25 TPa) [13], thermal conductivity ($(4.8–5.3) \times 10^3$ W/m K) [13], electrical conductivity (6000–7200 S/m) [15], specific surface area (theoretical

[1] The article is published in the original.

limit, ~2630 m^2/g) [14], high aspect ratio [16], low density (~2.28 g/cm^3) [17], low coefficient of thermal expansion (CTE) and high intrinsic mobility (2×10^5 $cm^2/(v\ s)$) [18]. The above-mentioned special properties of Gra have been nominated it as a suitable filler as reinforcement in PNCs [19]. Gra-reinforced PNCs have been successfully applied in a wide range of applications such as; photovoltaic devices, sensors [10], transparent electrodes [2], super capacitors, solar cells [2, 10], energy storage devices, packaging materials, antistatic coatings and especially in the nanocomposites [20–23]. The various reinforcing effects of Gra in PNCs based on a range of matrices such as polystyrene [24], polyurethane [25], polyaniline [26], poly(vinylidene fluoride) [27], epoxy [28] and etc., have been widely explored.

Epoxy is one of the mostly used thermoset polymers with a broad application range including coatings, electronic encapsulants, adhesives and matrix of PNCs because of its special characteristics such as high tensile strength and modulus, low shrinkage during curing process, good chemical and corrosion resistance, low cost and good processability [29–31]. However, the high viscosity and tight 3-dimensional chain structures of the highest performance epoxies could lead to a problem during PNCs fabrication process; an inherent brittle nature and consequently low crack resistance with limited usability in the mechanical parts. Numerous attempts have been done to improve the stiffness, toughness and strength of the epoxy resins by involving a second phase (nanofillers; with superior nature) along side of enhancing the mixability of these resins by adding diluting agents (organic solvents) before the fillers' addition to the matrix [32–35]. Investigations to improve the mechanical and physical properties of thermoset polymers have been revealed that the type of fillers and dispersion methods [36] as well as type of matrix [2] significantly affected the final properties of PNCs. M. Moazzami Gudarzi et al. [37] studied the various strategies of Gra dispersion in PNCs and concluded that the proper dispersion of Gra in epoxy matrix enhanced bonding between Gra and the matrix. Mohammad A. Rafiee et al. [34] and Shin-Yi Yang et al. [38] compared reinforcing characteristics of Gra in PNCs with CNTs and indicated that Gra could enhance the mechanical properties of the epoxy resins in the lower contents more significantly compared to CNTs. Additionally, Xin Zhao [13] and Tao Wang et al. [19] reported an acceptable improvement in the mechanical strength of PNCs. One of the most important advantages of the nanosized allotropes of carbon (such as graphene nanosheets (GNSs)) is its synergistic effect on intrinsic properties of the matrix. In another word, GNSs can be used in the PNCs with multifunctional behavior; where simultaneous enhanced mechanical and electrical properties are needed.

Through the current research, GNSs reinforced epoxy nanocomposites were prepared at various contents according to the related ASTM code. The aim of the present study was to investigate the reinforcement possibility and electrical resistivity reduction ability of GNSs as nanofillers. Unlike the majority of other works, bulk samples were used in much higher volumes through the present research. By increasing the size of the sample, the chance of having uniform distribution of the GNS reduces. So, two methods of solvent-free and solution methods (solvent-borne) were employed to distribute GNSs inside the epoxy matrix. The role of dispersed nanofillers within the matrix was analyzed to determine the electrical conductivity, tensile and flexural strengths. It was concluded that the electric conductivity of the sample could be good evidence of well distribution of the GNSs. The inner *d*-spacing of pristine GNSs was characterized by X-Ray diffraction (XRD). The dispersion state and morphology of GNSs in the prepared samples were characterized by the field emission scanning electron microscope (FE-SEM). In addition, the effect of dispersion state, solvent free and solvent-borne, on mechanical and electrical properties were discussed.

EXPERIMENTAL

Materials

Low viscosity DGEBA epoxy resin (ML-526) from the commercial mark of Mokarrar Engineering Materials Co. was used as the matrix. The stated-epoxy resin had good physical properties such as, low viscosity (1190 centipoise at 25°C), good mechanical properties, approximately no shrinking after curing and excellent filler wettability. Polymer matrix was prepared by mixing 100 parts by mass of epoxy resin (Bisphenol F-Aliphatic) with 15 parts of polyamine hardener (HA-11). Tetrahydrofuran (THF) with purity of >99.9% was purchased from Merck Co. GNSs with average particle diameters of 5 μm and thickness of 6–8 nm were supplied by XG Science Inc. (USA). Figure 1 depicts a FE-SEM image of as the supplied GNSs. Within the image, supplied GNSs have various dimensions in length.

Preparation of Composites

The GNSs/Epoxy nanocomposites were prepared by following the standard procedures. They were prepared by adding 0.05, 0.1, 0.25, and 0.5 wt % of GNSs to epoxy matrix with solvent-free and solvent-borne methods. Due to severe increase in viscosity, the preparation of nanocomposites with filler contents more than 0.5 wt % was so difficult. On solvent-free method, first the needed amount of neat GNSs;

depended on wt %, were added to epoxy resin and mixed by using a mechanical stirring (Heidolph RZR2102) with 2000 rpm for 10 min to ensure uniform distribution of nanofillers inside the resin. In order to break the residual aggregates and reaching to the complete dispersion, mixtures containing 0.05, 0.1, 0.25, and 0.5 wt % of GNSs were sonicated for 30, 210, 225, and 240 min, respectively at 200 W with a probe sonicator (14 mm diameter) (Hielscher Ultrasound Technology, UP400S). During the sonication, the mixture containing epoxy resin and nanofillers was prevented from over-heating by the aid of ice-bath around it. Since the two-dimensional nanofillers were similar to the CNTs or CNFs against sonication power, they were expected to be affected by increasing the sonication time. Figure 2a indicates the schematic illustration of this sample's preparation method.

In solvent-borne method, GNSs at the identical amounts as the solvent free method was initially mixed with tetrahydrofuran (THF) for 10 min at 2000 rpm and then subsequently sonicated with the same procedure as the solvent-free technique but in lower duration of times. After that, the epoxy was added to the mixture and the remaining sonication time was applied to disperse GNSs into the resin. To remove the solvent from the suspension, the mixture was vacuumed at 1 mbar for 1–2 h.

Then, hardener was added and gently stirred for 5 min. The mixtures were vacuumed for maximum 10 min at 1 mbar to remove any trapped air. Finally, the prepared samples (epoxy resin loaded GNSs) were poured into the standard molds for both tensile and flexure tests. All samples were cured for 48 h at room temperature followed by post-curing processes for 2 h at 80°C and 1 h at 110°C as per data sheet of epoxy. Dimension tolerance of the samples after exact polishing was ±0.1 mm. The schematic illustration of the solvent-borne procedure has been presented in Fig. 2b.

Characterization Techniques

Mechanical testing. All mechanical results were obtained using the Santam universal test machine (STM-150), which was equipped with a load cell in 10 KN capacity order. Figure 3 shows the mentioned machine with the test sample. The prepared GNSs/Epoxy nanocomposite samples and dimension of them have been shown in Fig. 4. ASTM-D 638 and D 790-03 were used for preparation and testing of flexure (Fig. 4a) and tensile (Fig. 4b) specimens, respectively. Based on the related standards, the average values of 5 tested specimens were reported.

Tensile tests of dog-bone shaped specimens (Fig. 4b) were performed at 25°C with a constant cross-head rate of 5 mm/min. Three-point bending tests were performed at the cross head motion of 16 mm/min with a 60 mm support span L in room temperature to measure the flexural properties (Fig. 4a). Flexural strength and moduli calculated with Eqs. (1) and (2), in MPa and GPa, respectively:

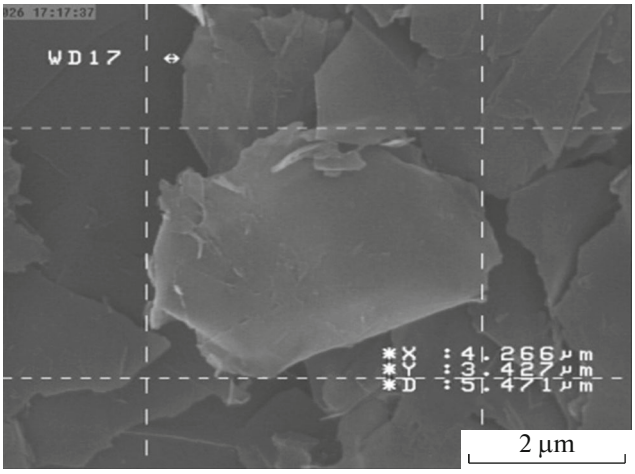

Fig. 1. FE-SEM image of as received graphene nanosheets (GNSs).

$$\sigma = 3PL/2bd^2, \quad (1)$$

$$E_B = L^3m/4bd^3, \quad (2)$$

where P is the load at a given point on the load-deflection curve in Newton (N), L is the support span length in mm, b and d are the width and depth of tested beam both in mm, and finally, m is the slope of the tangent to the initial straight-line portion of the load-deflection curve in N/mm.

Electrical testing. Measurement of the electrical resistivity of GNSs reinforced epoxy nanocomposites (produced by solvent free method) had done by using MI 3201TeraOhm 5 kV Plus having maximum input resistance of 1013 Ω. The composites were cut into rectangular bars with dimension of 20 mm × 20 mm × 2 mm (length, width and thickness). Copper sheets were stuck to the two surfaces of samples to ensure a full connection with electrodes. The measured resistivity was converted to conductivity by using Eq. (3):

$$\sigma_v = \frac{t}{R \times L^2}, \quad (3)$$

where σ_v is the volume conductivity, R is the bulk resistivity, t and L are the thickness and length of the electrical test specimen.

X-Ray diffraction pattern. Inter d-spacing of GNSs were determined using an X-ray diffractometer (XRD) (X'Pert, PHILIPS-PW 3040/60). XRD patterns were obtained conducting a CuK_α radiation ($\lambda = 0.154$ nm) with a step size of 0.02° at a scanning rate of

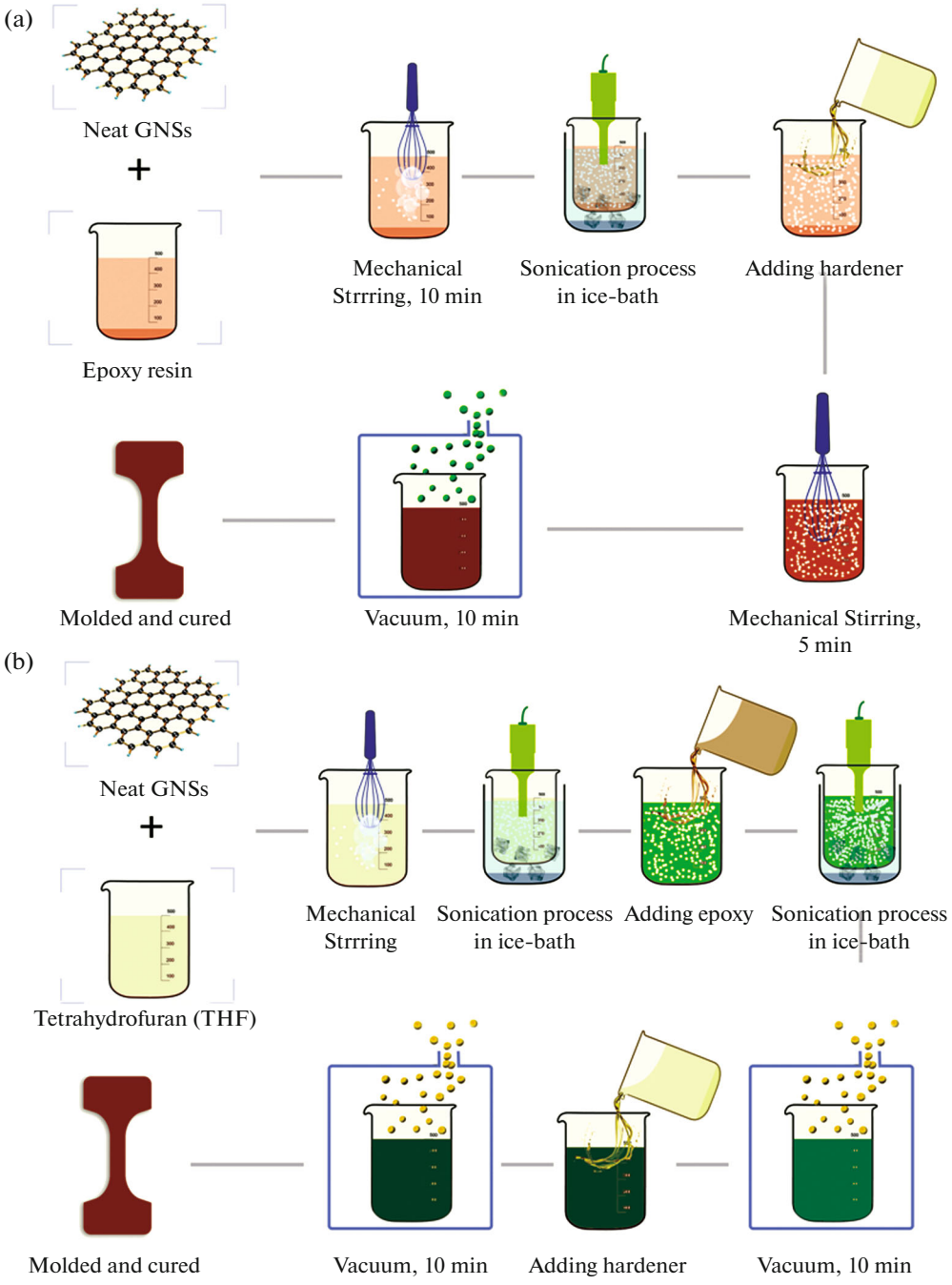

Fig. 2. (Color online) Schematic illustrations of sample preparation (a) using solvent free method and (b) using solvent-borne method.

0.6 deg/min, working at 40 kV 30 mA. It is relatively easy to determine the composition and crystal structure of the material from the positions (in degree) and relative intensities of the diffraction peaks. The XRD pattern of as received GNSs indicated an intense peak at a 2θ angle of 26.6°, corresponding to a basal spacing of 3.35 nm. The intense peak of graphite flakes is so sharp in comparison with GNSs intensity [39].

Electron microscopy characterization. Field emission scanning electron microscope, FE-SEM (Hitachi, Japan S-416), operating at 15 kV, was used to characterize the dispersion state of nanofillers and analyze the fractured surface morphology of the prepared samples after the mechanical tests. The fractured surfaces were coated with gold for 5 min (thickness of 10 Å) using a Technics Hi-coater.

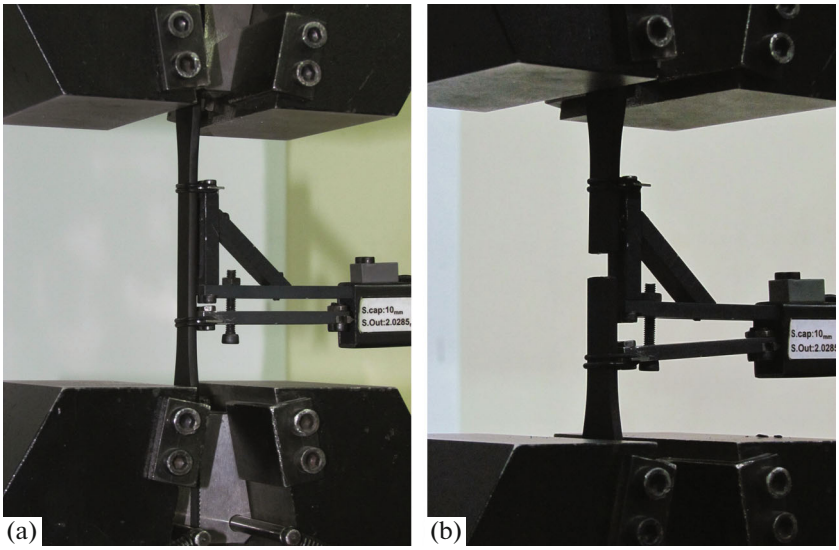

Fig. 3. (Color online) Santam universal test machine (STM-150) during sample testing, (a) before and (b) after test.

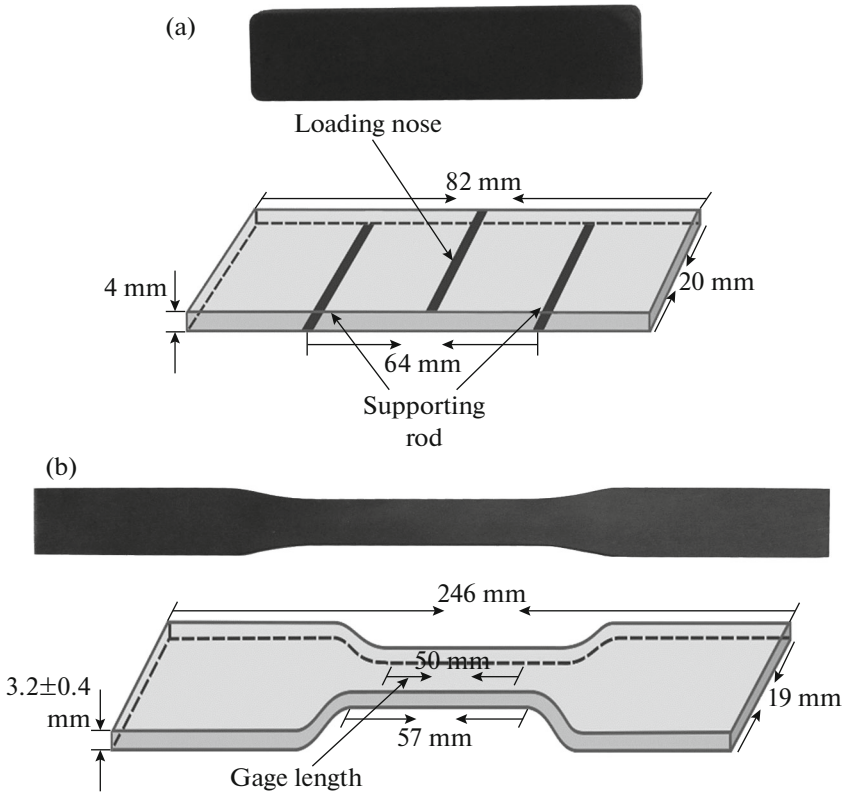

Fig. 4. As prepared (a) flexural and (b) tensile specimens and the standard dimension of them.

RESULTS AND DISCUSSION

Analysis of Variance of the Experimental Data

Two-way ANOVA was performed in order to survey the significance of the experimental results. To aim this goal, two groups of experimental data for "solvent free" and "solvent borne" methods were considered. Each group (say processing method) was prepared using five different amounts of GNSs content, and each experiment had three replications. The results of ANOVA analysis for strength and modulus of the samples have been presented in Tables 1 and 2.

Table 1. Two-factor ANOVA for flexural strength data

SUMMARY	Count	Sum	Average		Variance	
Solvent free	5	563.3	112.66		5.503	
Solvent borne	5	537.1	107.42		2.392	
Source of variation	SS	df	MS	F	P value	F crit
Methods (solvent free/borne)	68.644	1	68.644	154.6036	0.000241	7.708647
GNS contents	29.804	4	7.451	16.78153	0.009132	6.388233
Error	1.776	4	0.444			
Total	100.224	9				

Table 2. Two-factor ANOVA for flexural modulus data

SUMMARY	Count	Sum	Average		Variance	
Solvent free	5	14.88	2.976		0.01483	
Solvent borne	5	15.92	3.184		0.01403	
Source of variation	SS	df	MS	F	P value	F crit
Methods (solvent free/borne)	0.10816	1	0.10816	157.8978	0.000231	7.708647
GNS contents	0.1127	4	0.028175	41.13139	0.001663	6.388233
Error	0.00274	4	0.000685			
Total	0.2236	9				

In ANOVA method, the high F values indicated that the studied parameters had significant effect on the goal parameter. As it is obvious from Tables 1 and 2, the F values are much higher for alters in the processing method than for variations in GNSs content; which means that, the processing method had the major influence on the flexural strength and modulus parameters. According to Tables 1 and 2; the P-values for both alterations in processing method and variation in GNSs content is lower than 0.05; that reveals, both parameters had a significant effect on the flexural strength and modulus parameters.

Tensile Properties

The reinforcing effect of dispersed GNSs with different contents using two dispersion methods inside the epoxy resin has been investigated. Stress-strain curves and Young's moduli results of the investigated samples are presented in Fig. 5. Through the previous work, the present researchers studied the mechanical properties enhancement of epoxy-based composites using CNTs as reinforcement and found that carbon based nanofillers had the proper ability to enhance the mechanical properties of PNCs [40]. Figure 5 shows how addition of GNSs in solvent-free and solvent-borne media have affected the tensile strength and Young's modulus of the pristine epoxy resin matrix. As it can be seen, introducing GNSs into epoxy in solvent free method gets in the hand relatively better improvement in comparison with the solvent-borne method. Figures 5a–5e show that addition of GNSs at a very low weight ratio (0.1 wt %) has increased the tensile strength by about 15% in solvent-free method, while it was about 10% for solvent-borne procedure. In low filler contents, it is easy to separate GNSs from each other and disperse them inside the polymeric chains (Figs. 6a and 6b). On the other hand, at higher GNSs contents, the tensile strength demonstrates a decreasing trend which may be due to the severe agglomerations of GNSs (Figs. 6c, 6d). Unlike the strength, the Young's moduli of the prepared nanocomposites were increased up to 2.82 and 2.75 GPa, as weight percent was increased in both solvent free and solvent-borne procedures (about 12 and 10% improvement, respectively) (Fig. 5f). Consequently, the lower improvement that was observed for the tensile properties of compos-

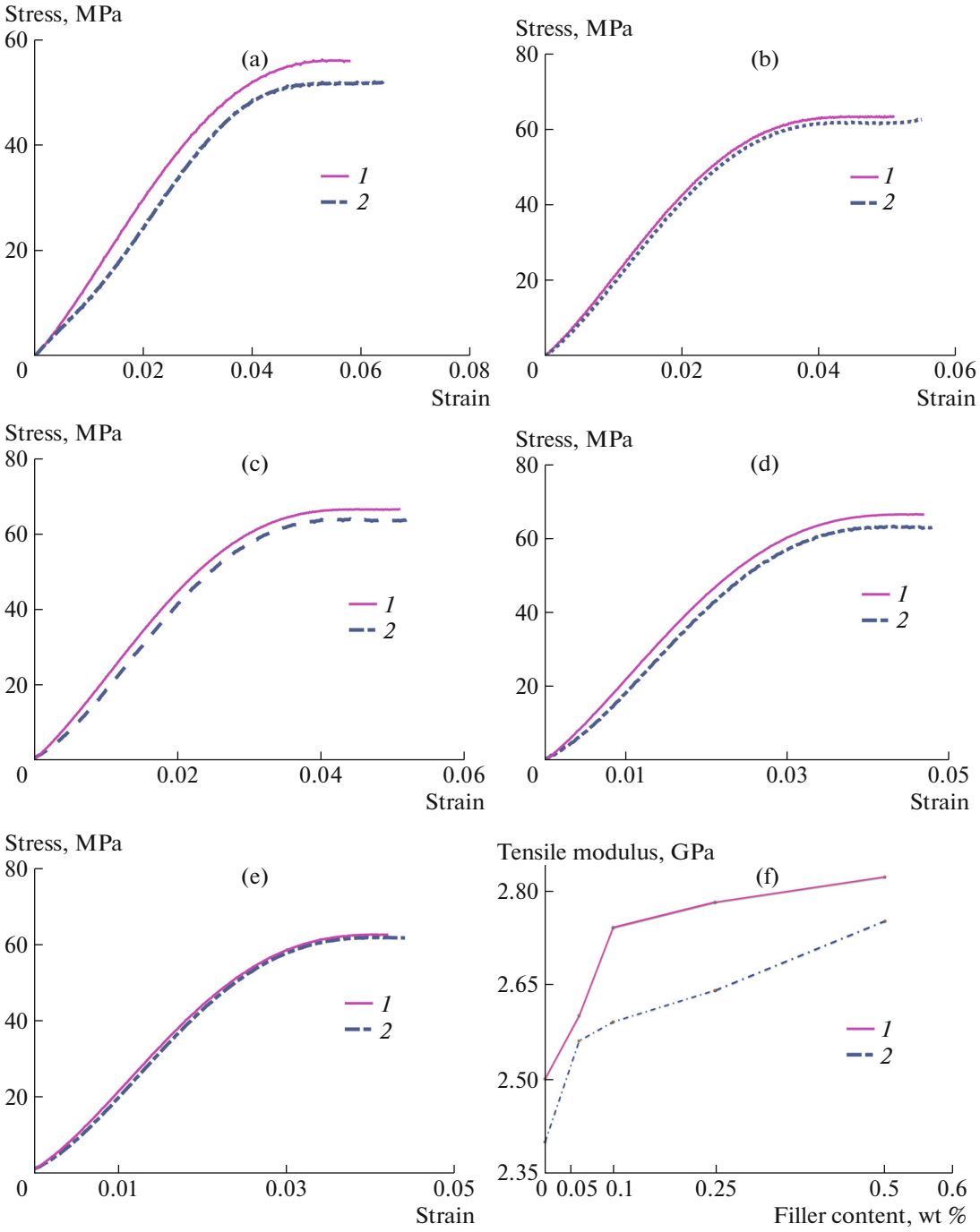

Fig. 5. (Color online) The stress-strain curves of the samples containing (a) 0, (b) 0.05, (c) 0.1, (d) 0.25, (e) 0.5 wt % of graphene nanosheets (GNSs) and (f) Young's modulus of the GNSs/Epoxy nanocomposites. (*1*) Solvent free, (*2*) solvent borne.

ites with GNSs may be attributed to three reasons as follows:

(I) Restacking and aggregation of nanosheets;

With increasing filler content, there will be no space for proper dispersion and thus GNSs will be in Van der Waals force domains of each others, so the GNSs will stick together and form agglomerates if more GNSs stick together. As a result, the role of the reinforcement as well as the efficient volume will be reduced. This process, in higher loading amount, especially when the dispersion of nanofillers in bulk quantities is required, decreases the strength values even to lower than neat matrix strength. These formed agglomerates, thereby causing initial crack growth and easy crack branching. As the agglomerations are stress

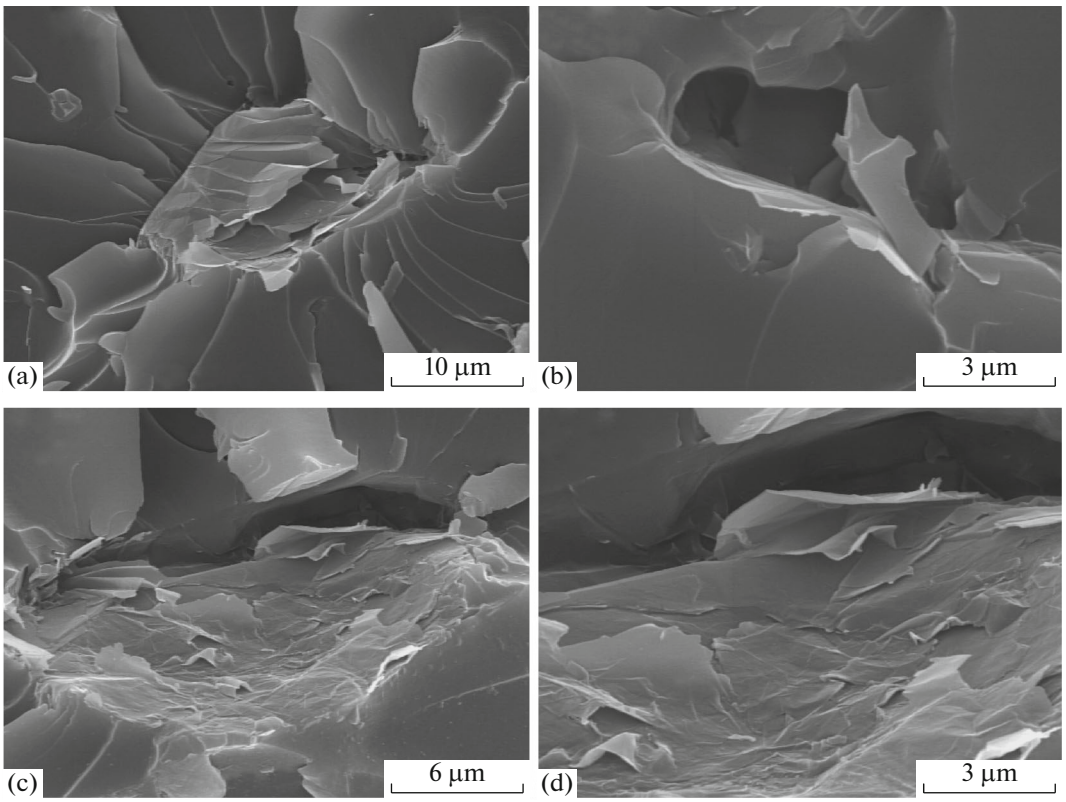

Fig. 6. (a, b) Graphene nanosheets (GNSs) imprint on fracture surface of 0.1 wt % and (c, d) remaining agglomerates inside the matrix reinforced with 0.5 wt % GNSs dispersed with solvent free procedure, GNSs were completely impregnated with epoxy resin matrix.

concentration points, so these are the most important reasons of strength reduction.

(II) Voids: In viscous polymer matrices and high filler loading conditions, even with long vacuuming before the molding, they will not vanish.

(III) Geometry, aspect ratio and interface interaction of the nanofillers.

Considering these probable reasons, it could be concluded that the final properties of the achieved composites were influenced by the characteristics and geometry of filler type. Among these reasons, the cases (I) and (II) are responsible for cracks, where the negative effect of agglomerates is higher than the voids.

The FE-SEM images of the fractured surface of the prepared PNCs (Fig. 6) clearly indicated that agglomerates were the main reasons of strength reduction. Regardless of dispersion methods, an optimum dispersion of GNSs inside the polymeric matrix was observed on the fractured surfaces of the samples with low filler content (Figs. 6a, 6b), while with increasing filler content the agglomerates could not fully be avoided (Figs. 6c, 6d). In Figs. 6a, 6b, it is clear that during the tensile test some nanosheets of Gra, bear tensile strength, where one end of them are drawn (pulled out). According to these images, it could be concluded that the main strengthening mechanism at low filler contents is pulling-out of GNSs.

Flexural Properties

Flexural modulus and strength of GNSs/Epoxy nanocomposites were also studied in order to evaluate the reinforcement role of GNSs under the bending stresses. Flexural properties were very similar to the tensile properties. However, the flexural properties enhancement was lower than the tensile strengths. Figure 7a presents the bending strength of the prepared PNCs. It is obvious that the addition of a slight amount of GNSs (0.1 wt %) increased the flexural strength and modulus in solvent free method (Fig. 7b) by about 5 and 7 percent, respectively. Unlikely, the solvent-borne results were indicated that employing solvent decreased the flexural properties (and also tensile strengths) at any filler contents. In addition, it is valuable to notice that the addition of solvent has decreased the intrinsic mechanical properties of the pristine epoxy resin. For the aim of comparison, when processing 0 wt % GNSs samples using solvent borne method, 0 wt % GNSs content of the solvent has been

added to the mixture in order to study the effect of adding solvent itself. As it can be concluded from Fig. 7, for 0 wt % GNSs loadings, the samples processed using solvent-free method had superior properties in comparison to the solvent borne method. Given the fact that in solvent borne method the mixture was vacuumed at 1 mbar for 1–2 h in order to completely remove the solvent from the suspension, it could be inferred that adding solvent had adverse effect on the matrix polymer, where by adding solvent adverse interactions caused to the considerable reduction in characteristics of the product.

As indicated, all investigated properties of the solvent-borne method were less than that of solvent-free procedure, which revealed that using solvent had negative effects on the mechanical properties of the prepared nanocomposites and did not enhance the dispersion of GNSs unlike some reports [34, 41]. The indicated negative effect might be due to the participation of the applied solvent in the polymerization and cross-linking of the matrix resin (like the effect of styrene in polyester or vinylester medium). Furthermore, the negative impact in the strength properties would be due to (1) the lack of complete removal of the solvent from the prepared PNCs even after the vacuum process, (2) unwanted and undesirable interactions between the solvent and matrix polymeric chains. The last case is more possible because, in the present study, special care was done in order to completely remove the solvent before adding hardener. According to Figs. 5 and 7, both tensile and flexural strengths were increased initially, but after reaching its optimum decreased with increasing the filler contents. Existing of an optimum point for the strength properties was inevitable due to the dispersion problems. This issue is important, especially when the bulk quantity of nanofillers should be dispersed.

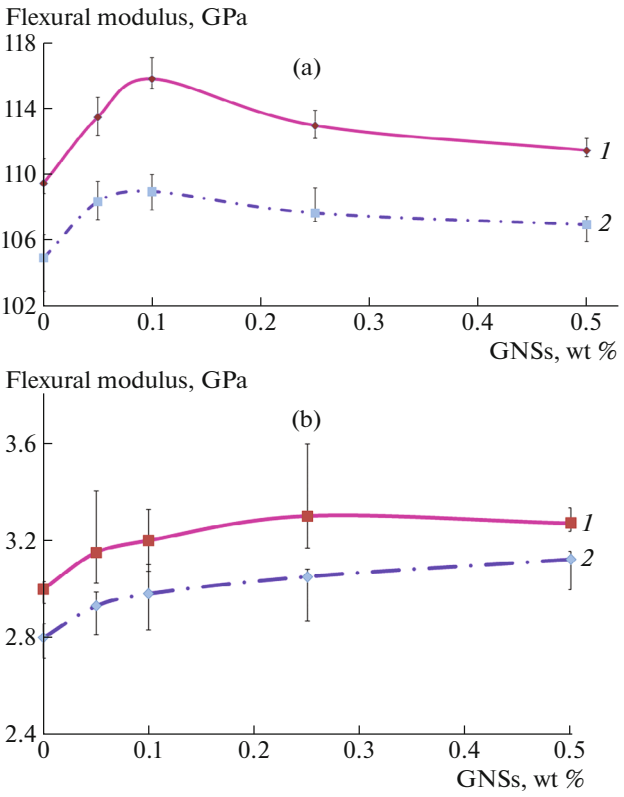

Fig. 7. (Color online) (a) Flexural strength and (b) flexural modulus curves of the graphene nanosheets (GNSs)/Epoxy nanocomposites. (*1*) Solvent free, (*2*) solvent borne.

Dispersion and Fracture Surface Analysis

The nanofiller dispersion quality in the polymeric matrix directly correlates with its effectiveness for improving the mechanical, electrical and thermal properties. Here, it was investigated the dispersion of GNSs and the morphology of the fractured surfaces of epoxy composites using FE-SEM (Fig. 8). Morphology of the fractured surfaces showed that with increasing the filler content, fractured surface would be rougher. Roughness was indicative of deflection of cracks during propagations on the fractured cross section. As it is well known, crack deflection is one of the strengthen mechanisms. Crack deflection in Gra nanocomposites compared to the nanocomposites of CNFs and CNTs is very common. Also, GNSs with high aspect ratio had much more impressive strengthen effects. So nanocomposites of Gra compared to composites of one-dimensional nanofillers would have further strengthen properties. However, many other parameters especially lack of proper dispersion prevented achieving the mentioned-peak due to Van der Waals forces inside the Gra sheets.

Comparing Figs. 6a–6d indicates that if the amount of GNSs loading would be less in the composites, the proper dispersion inside the matrix network chains would be possible due to the existing of higher free spaces, while with increasing the nanofiller contents, due to the lack of these spaces, separating all particles (sheets) from each other would not be possible. Additionally, spread GNSs had re-aggregation potential and it would be possible to form agglomerates (Figs. 6c and 6d). In the present study, producing species with more than 0.5% weight percent of nanofillers were not possible. Because it was observed that, as the nanofiller contents percentage increased, the fluidity of the matrix strongly decreased, due to the filling of all free spaces, which saturating all parts inside the chains and they could not move. So in this case, dispersion and even molding was not possible without avoiding voids due to loss of fluidity.

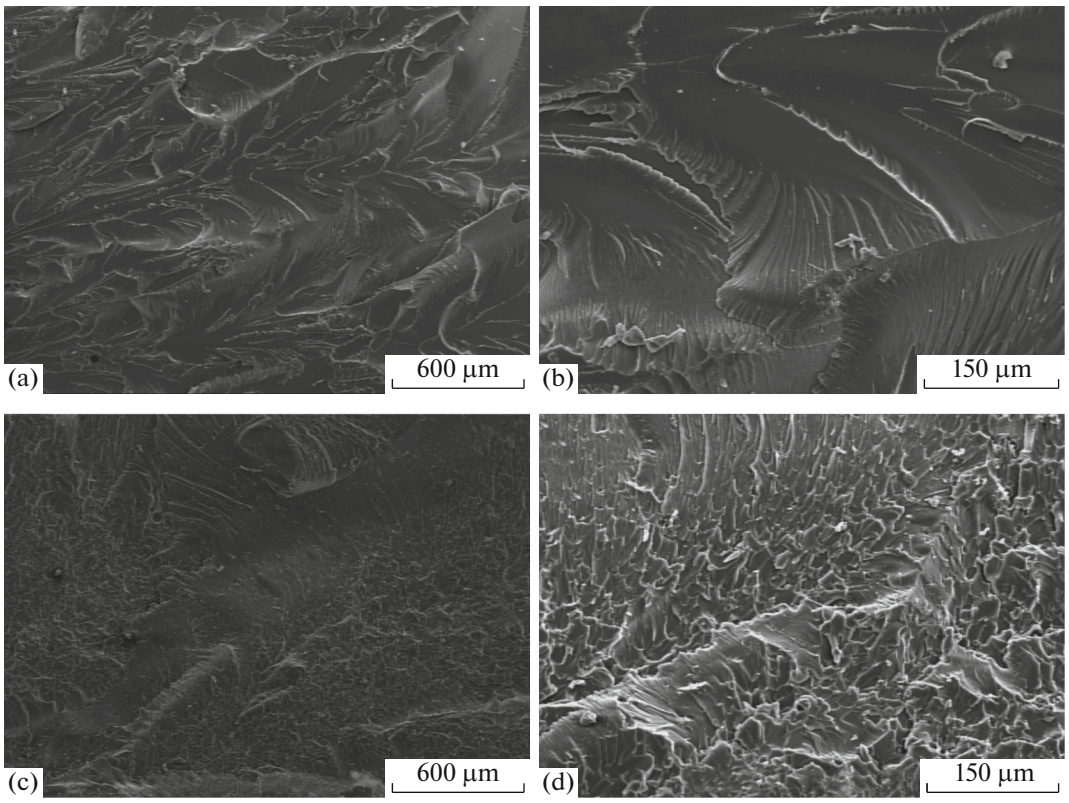

Fig. 8. Micrograph of neat and graphene nanosheets (GNSs) reinforced epoxy resin: (a, b) neat epoxy resin, (c, d) 0.1 wt % GNSs-filled epoxy resin at the same magnifications.

Electrical Properties

Unlike the mechanical properties, no significant difference was observed in the electrical resistivity at low filler contents. Figure 9 shows the electrical conductivity versus weight percentage of GNSs in the GNSs/Epoxy nanocomposites. According to Fig. 9, it is obvious that the electrical conductivity of the prepared nanocomposites was exhibited percolation behavior. Here, as it is obvious, percolation threshold achieved at 1 wt % of filler content. The conductivity of the neat epoxy resin was less than 10–12 S/cm and at GNSs loading up to 0.5 wt %, the composite did not show any considerable value. It was expected that by increasing the weight percent of GNSs, the electrical conductivity was also raised, although after crossing the percolation threshold the gradient reduced. The electrical conductivity increased by 7 orders of magnitude for composites with GNSs higher than 1 wt % and then plateaus as could be seen from Fig. 9. GNSs coming into contact with each other and forming conductive pathways throughout the neat epoxy matrix chain networks at high GNSs loading which was considered as a possible reason for improvement in the electrical conductivity. Conduction mechanism in PNCs is very complicated, and many factors could affect the electrical conductivity and should be considered during preparation of conductive polymer composites (CPCs).

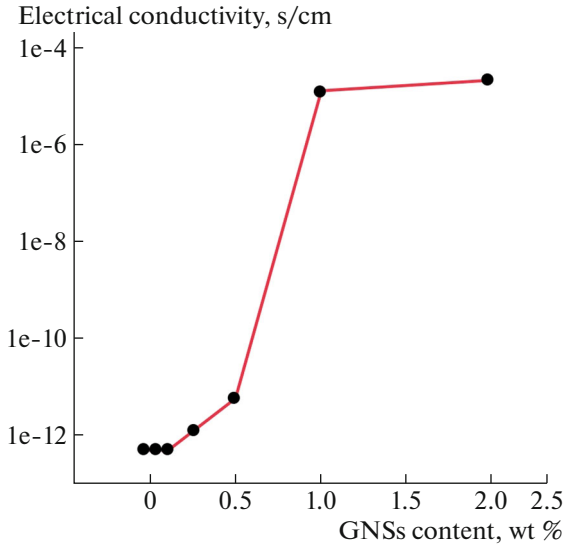

Fig. 9. (Color online) The electrical conductivity versus conductive filler content for the graphene nanosheets (GNSs)/Epoxy nanocomposites.

The main parameters that can influence the formation of conductive networks inside the polymer chains are dimension and geometry of nanofillers, type of matrix including polarity and condition of chain arrangement, method and process of dispersion. Due to 2-dimensional geometry of Gra in comparison of 1-dimension geometry of other fillers such as CNTs and CNFs, it is expected that the percolation threshold of GNSs composites occurs in less amount than of 1-dimensional fillers reinforced composites. However, Jinhong Du et al. [42] reported that, in contrary to the theoretical predictions, the GNSs/high density polyethylene (HDPE) composites showed much higher percolation threshold and lower electrical conductivity than the MWCNTs/HDPE composites. It could be concluded that the high percolation threshold which was achieved in the current study could be because of the lack of proper dispersion and agglomerates creation that reduced the fillers effective volume within the matrix.

CONCLUSIONS

The GNSs/Epoxy nanocomposites using two solvent free and solvent-borne procedures were prepared through the current study. The tensile and flexural properties as well as the electrical conductivity of the prepared nanocomposites were investigated. Mechanical characterization of the prepared specimens, demonstrated an increase in ultimate tensile and flexural strengths for low GNSs loadings up to 0.1 wt %, accompanied with continuous increase in both Young's and flexural modulus. The solvent-borne nanocomposites showed different results despite the same treatment that held to prepare GNSs/epoxy nanocomposites. In these samples, the tensile strength reached to its maximum value at 0.1 wt % of filler contents, but still that was lower than the values for solvent free procedure. Besides that, the flexural values were considerably lower than the pristine epoxy resin in these samples. The electrical conductivity measurements illustrated that the conductivity was enhanced as the filler loading increased and the electrical percolation threshold was achieved at 1 wt % of GNSs. FE-SEM images demonstrated that pull-out mechanism was the main reason for reinforcing the prepared nanocomposites. In addition, the results showed that improvements in the mechanical properties could be observed just at low filler contents, which could be due to the reason that, at higher filler contents, it was not possible to remove any agglomerates inside the compacted polymer chains. Thereby, it is believed that there always be critical filler loading which after that the mechanical properties, especially the strength decreases because of the agglomeration.

REFERENCES

1. S. Iijima, Nature **354**, 56(1991).
2. T. Kuilla, S. Bhadra, D. Yao, N. H. Kim, S. Bose, and J. H. Lee, Prog. Polym. Sci. **35**, 1350 (2010).
3. A. K. Geim and K. S. Novoselov, Nat. Mater. **6**, 183 (2007).
4. K. Osouli-Bostanabad, E. Hosseinzade, A. Kianvash, and A. Entezami, Appl. Surf. Sci. **356**, 1086 (2015).
5. K. Osouli-Bostanabad, H. Aghajani, E. Hosseinzade, H. Maleki-Ghaleh, and M. Shakeri, Mater. Manuf. Processes **31**, 1351 (2016).
6. R. He, Q. Chang, X. Huang, and J. Li, Mech. Compos. Mater. **53**, 753 (2018).
7. T. Ishikawa, Adv. Compos. Mater. **15**, 3 (2006).
8. M. T. T. Huynh, H.-B. Cho, T. Suzuki, H. Suematsu, S. T. Naguyen, K. Niiihara, and T. Nakayama, Compos. Sci. Technol. **154**, 165 (2018).
9. J. G. Zhang, Mech. Compos.Mater. **47**, 447 (2011).
10. V. Singh, D. Joung, L. Zhai, S. Das, S. I. Khondaker, and S. Seal, Prog. Mater. Sci. **56**, 1178 (2011).
11. H. Kim, A. A. Abdala, and C. W. Macosko, Macromolecules **43**, 6515 (2010).
12. J. Kim, B.-S. Yim, J.-M. Kim, and J. Kim, Microelectron. Reliab. **52**, 595 (2012).
13. X. Zhao, Q. Zhang, D. Chen, and P. Lu, Macromolecules **43**, 2357 (2010).
14. S. G. Prolongo, R. Moriche, A. Jiménez-Suárez, M. Sánchez, and A. Ureña, Eur. Polym. J. **61**, 206 (2014).
15. D.-W. Wang, F. Li, J. Zhao, W. Ren, Z.-G. Chen, Z.-Sh. Wu, I. Gentle, G. Q. Lu, and H.-M. Cheng, ACS Nano **3**, 1745 (2009).
16. B. Ahmadi-Moghadam, M. Sharafimasooleh, S. Shadlou, and F. Taheri, Mater. Des. **66**, 142 (2015).
17. H.-B. Zhang, W.-G. Zheng, Q. Yan, Y. Yang, J.-W. Wang, A.-H. Lu, G.-Y. Ji, and Z.-Z. Yu, Polymer **51**, 1191 (2010).
18. Y. Zhu, S. Murali, W. Cai, X. L. J. W. Suk, J. R. Potts, and R. S. Ruoff, Adv. Mater. **22**, 3906 (2010).
19. T. Wang, M. D. J. Quinn, and S. M. Notley, Carbon **129**, 191 (2018).
20. S. Gantayat, D. Rout, and S. K. Swain, Polym.-Plast. Technol. Eng. **57**, 1 (2018).
21. R. Sun, L. Li, C. Feng, S. Kitipornchai, and J. Yang, Eur. Polym. J. **98**, 475 (2018).
22. R. J. Young, M. Liu, I. A. Kinloch, S. Li, X. Zhao, C. Vallés, and D. G. Papageorgiou, Compos. Sci. Technol. **154**, 110 (2018).
23. Y. Li, S. Wang, Q. Wang, and M. Xing, Composites, Part B **133**, 35 (2018).
24. J. Zhao, Y. Liu, J. Cheng, S. Wu, Z. Wang, H. Hu, and C. Zhou, Polym. Int. **66**, 1827 (2017).
25. Y. Li, F. Gao, Z. Xue, Y. Luan, X. Yan, Z. Guo, and Z. Wang, Mater. Des. **137**, 438 (2018).

26. A. Hazarika, B. K. Deka, K. Kong, D. Y. Kim, Y.-W. Nam, J.-H. Choi, C.-G. Kim, Y.-B. Park, and H. W. Park, Composites, Part B **140**, 123 (2018).
27. F.-C. Chiu, Y.-C. Chuang, S.-J. Liao, and Y.-H. Chang, Polym. Test. **65**, 197 (2018).
28. A. Bisht, K. Dasgupta, and D. Lahiri, J. Appl. Polym. Sci. **135**, 46101 (2018).
29. C. May, *Epoxy Resins: Chemistry and Technology* (Marcel Dekker, Inc., New York, 1987).
30. K. Osouli-Bostanabad, A. Tutunchi, and M. Eskandarzade, Int. J. Adhes. Adhes.**75**, 145 (2017).
31. A. Tutunchi, R. Kamali, and A. Kianvash, Soft Mater. **14**, 1 (2016).
32. Y. S. Song and J. R. Youn, Carbon **43**, 1378 (2005).
33. E. T. Thostenson and T.-W. Chou, Carbon **44**, 3022 (2006).
34. M. A. Rafiee, J. Rafiee, Z. Wang, H. Song, Z.-Z. Yu, and N. Koratkar, ACS Nano **3**, 3884 (2009).
35. L.-C. Tang, Y.-J. Wan, K. Peng, Y.-B. Pei, L.-B. Wu, L.-M. Chen, L.-J. Shu, J.-X. Jiang, and G.-Q Lai, Composites, Part A **45**, 95 (2013).
36. B. Liand and W.-H. Zhong, J. Mater. Sci. **46**, 5595 (2011).
37. M. M. Gudarzi and F. Sharif, eXPRESS Polym. Lett. **6**, 1017 (2012).
38. S.-Y. Yang, W.-N. Lin, Y.-L. Huang, H.-W. Tien, J.-Y. Wang, C.-C. M. Ma, S.-M. Li, and Y.-S. Wang, Carbon **49**, 793 (2011).
39. S. H. Aboutalebi, M. M. Gudarzi, Q. B. Zheng, and J.-K. Kim, Adv. Funct. Mater. **21**, 2978 (2011).
40. F. Vahedi, H. R. Shahverdi, M. M. Shokrieh, and M. Esmkhani, Carbon **29**, 419 (2014).
41. U. Khan, P. May, A. O'Neill, and J. N. Coleman, Carbon **48**, 4035 (2010).
42. J. Du, L. Zhao, Y. Zeng, L. Zhang, F. Li, P. Liu, and C. Liu, Carbon **49**, 1094 (2011).